Cell-specific nitrogen responses mediate developmental plasticity

Miriam L. Gifford*†, Alexis Dean*, Rodrigo A. Gutierrez*‡, Gloria M. Coruzzi*, and Kenneth D. Birnbaum†§

†Center for Genomics and Systems Biology and *Department of Biology, New York University, 100 Washington Square East, New York, NY 10003; and ‡Departamento de Genética Molecular y Microbiología, Pontificia Universidad Católica de Chile, Alameda 340, Santiago 8331010, Chile

The organs of multicellular species consist of cell types that must function together to perform specific tasks. One critical organ function is responding to internal or external change. Some cell-specific responses to changes in environmental conditions are known, but the scale of cell-specific responses within an entire organ as it perceives an environmental flux has not been well characterized in plants or any other multicellular organism. Here, we use cellular profiling of five *Arabidopsis* root cell types in response to an influx of a critical resource, nitrogen, to uncover a vast and predominantly cell-specific response. We show that cell-specific profiling increases sensitivity several-fold, revealing highly localized regulation of transcripts that were largely hidden from previous global analyses. The cell-specific data revealed responses that suggested a coordinated developmental response in distinct cell types or tissues. One example is the cell-specific regulation of a transcriptional circuit that we showed mediates lateral root outgrowth in response to nitrogen via microRNA167, linking small RNAs to nitrogen responses. Together, these results reveal a previously cryptic component of cell-specific responses to nitrogen. Thus, the results make an important advance in our understanding of how multicellular organisms cope with environmental change at the cell level.

cell sorting | microRNA | lateral roots | auxin response | transcriptional analysis

Individual cell types differ dramatically in their transcriptional programs on a global level (1–3). Thus, to deconvolute the genetic programs that mediate development, it is necessary to separate signals from different cells to discriminate the genes that determine cell fate and specificity. Similarly, cells are known to respond individually to environmental inputs, and identifying cell-specific responses on a global scale is critical to understanding how organs partition functions among cell types. We provide a high-resolution readout of an organ-level response by exposing whole roots to an environmental stimulus and identifying responses in individual cell types by analysis of expression profiles before and after treatments.

For plants, reactions to environmental stimuli are particularly important, because they are sessile yet must still cope with changes in the environment. The root's response to nitrogen is an ideal model to study how an organ reacts to environmental change, because nitrogen is a limiting resource for plants (4), and among the root's critical functions are the efficient uptake and utilization of nitrogen. Although a few genes are known to respond specifically to nitrogen in a subset of cells (5, 6), obtaining a comprehensive view of cell-specific reactions to an input in an entire organ has not been accomplished.

Results

Cell Sorting Yields an Accurate Readout of Environmental Responses at the Cell Level. We asked how the plant regulates transcription at the cellular level in response to nitrogen by adapting techniques used to generate static profiles of cells (1, 2). In brief, we treated cell-specific GFP-expressing plants with nitrate or control treatments, isolated individual cell types by a combination of protoplast generating treatment and FACS, and analyzed gene expression using microarrays (*Materials and Methods*).

To model a fluctuating soil environment, we grew plants for 12 days in 0.5 mM ammonium succinate, during which time nitrogen assays revealed a gradual depletion but not a complete exhaustion of nitrogen from the media (*Materials and Methods*), which avoids pure stress responses. Roots were then treated with 5 mM nitrate to mimic a nitrogen influx (7). The growing conditions and nitrogen treatments were selected based on known nitrogen responses and tested treatment regimes that best preserved nitrogen responses during protoplast-generating treatment (supporting information (SI) *Text*). Because one goal was to associate metabolic and cellular responses to developmental functions, we also chose treatment conditions that led to dramatic changes in plant architecture via root branching, which is mediated by the outgrowth of lateral roots from a subset of pericycle cells called founder cells. For cell sorting, roots were exposed to nitrate or mock (KCl) treatments for a total of 3.5 h and then isolated by FACS after a rapid enzymatic dissociation of cells (1, 2).

The goal of the analysis was to gain a comprehensive view of how tissues respond individually and coordinate their responses to nitrogen signals. Thus, five markers were selected to cover a range of cell types from inner to outer layers: lateral root cap and epidermis/cortex lines for cells that contact the soil, endodermis/pericycle and stele lines for cells that have a role in controlling vascular loading to the shoot, and pericycle founder cells, including initiating and preemergent lateral roots for cells that give rise to lateral appendages (*SI Text* and SI Fig. 5). In each case, we confirmed that we were able to generate protoplasts from the cell types marked by our fluorescent lines.

We used a two-way ANOVA to classify genes as responsive either to nitrogen across all cells (treatment level, $P < 0.05$) or only in specific cell types (cell × treatment interaction, $P < 0.05$). Responses in individual cells were identified by using a nonparametric test that accounted for multiple testing [significance analysis of microarrays (SAM) with a false discovery rate (FDR) of $q < 5\%$] (8) (SI Table 1).

To validate that cell-sorting techniques captured *in vivo* gene expression, we first confirmed that the cell-specific expression pattern of known root markers was recapitulated in our sorted cell treatment controls (1) (SI Table 3). We also confirmed the

PLANT BIOLOGY

Fig. 1. The root's response to nitrogen is highly cell-specific. (*a*) A heatmap showing all of the major patterns of nitrogen responses by classifying individual cell type or tissue responses as either induced, repressed or unchanged by nitrogen treatment. All patterns with more than five genes are shown. Patterns are ordered by clustering on Euclidean distance. (*b–d*) Average log^2 microarray expression values for three representative gene response clusters in control and treated experiments. Asterisks represent cell types in which all genes in the cluster showed a significant response (*SI Text*). (*b*) A spatially broad responsive group (cluster 1, *n* = 453). (*c*) A lateral root cap and pericycle-induced group (cluster 13, *n* = 942). (*d*) An epidermis/cortex repressed group (cluster 8, *n* = 40). (*e*) Diagram depicts the *Arabidopsis* root showing the five cell populations studied.

nitrogen response of two genes, *ATGSR* (9), which is broadly induced, and *ARF8*, which is induced in the pericycle and lateral root cap and marginally repressed in the stele (see below), using cell-specific GFP and GUS reporters, respectively (SI Fig. 8). In addition, we retested 10 genes that showed cell-specific but not whole-root responses in microarray analyses with more sensitive quantitative PCR (qPCR) assays on whole-root samples (SI Fig. 9, SI Table 4). All 10 transcripts showed the response predicted by cell sorting using qPCR on whole roots. Overall, these results confirm the accuracy of the cell sampling techniques in capturing the *in vivo* dynamics of cell types in response to nitrogen on a global scale.

The Plant Has a Vast Cell-Specific Response to Nitrogen That Has Not Been Previously Detected. The global results show that the vast majority of responses to nitrogen were cell-specific, demonstrating that the response to nitrogen is remarkably fine-tuned within the root (Fig. 1). We found a total of 5,396 transcripts (87%) of responding genes were significantly regulated in at least one, but not all, cell types profiled (Fig. 1*a*, clusters 2–28). Only 771 transcripts responded across all cell types examined (Fig. 1*a*, clusters 1 and 29). This large response also suggested that cell sorting greatly increased sensitivity to detect transcriptional regulation.

To ask whether cell sorting uncovered previously undetected

responses, we compared our cell-sorting results with the responses found in all comparable previously published transcriptome analyses on nitrogen responses (7, 10, 11) and a series of profiles we generated on whole roots using the same treatments as sorted cells. After standardizing the analysis of all experiments and setting liberal criteria to detect as many genes as possible [dChip normalization, t test filter ($P < 0.05$), FDR analysis ($q <$ 5%)], we found that cell sorting uncovers a much larger response than the 1,000–2,000 nitrogen-responsive genes reported in previous studies or found in our own whole-root experiments. This corroborates the increased sensitivity of the technique. A total of 4,139 genes were detected in all four studies, only 1,271 of which overlapped with the response detected by cell sorting. Thus, cell sorting uncovered an aspect of whole-genome responses to nitrogen treatments that are missed in whole-root studies.

The increased sensitivity of cell sorting was due to the ability to detect highly localized responses within the root that would have been diluted in whole-organ samples. In addition, cell sorting was able to detect transcripts with mixed induction and repression responses that, when combined, dampen strong signals from specific cells. For example, among genes induced by nitrogen treatment, transcriptional responses detected by both whole-root and cell-specific analyses were relatively broadly expressed (3.5 of 5 tissues on average), whereas those uniquely identified by cell sorting had a significantly narrower expression pattern on average (2.4 of 5 tissues, Student's t test, $P < 1E–12E$). In addition, more than half the genes detected in cell sorting (3,656) were induced in one cell type and repressed in another. The vast majority of these genes (85%) were not detected in any of the whole-root experiments. Thus, cell sorting provides a greatly expanded resource to study nitrogen responses (i.e., 4,931 of 6,202 gene responses were detected only by cell sorting) and uncovers a previously undocumented level of cell-specific responses in a multicellular organism on a global scale.

Nitrogen Elicits Coordinated but Distinct Cellular Responses in Different Tissues. One test of the utility of cell sorting is whether it can identify new types of functional responses. Gene Ontology (GO) provides one objective benchmark for the ability to classify genes into functional groups. Of 105 GO categories overrepresented in the various cell-specific response clusters, ≈50% ($n =$ 51) were not detected in our global whole-root response profiles. As expected, these unique functional categories were largely restricted to highly tissue-specific clusters. Although categories identified in whole-root responses were largely physiological and metabolic cellular processes, cell sorting tended to identify more specific processes [e.g., hormone-mediated signaling, cluster 25, $P < 0.05$; enzyme linked receptor protein signaling pathway, cluster 7, $P < 0.02$; response to light stimulus, cluster 8, $P < 0.002$ (Fig. 1d)].

Having evidence that response clusters captured spatially discrete functional responses to nitrogen, we used cell-specific responses to ask how broad signals might coordinate the effects of an influx of nitrate in different parts of the root. One set of candidate signals are plant hormones that can induce different metabolic and developmental responses in different parts of the root (12, 13). To identify tissues that might be responding to local hormone signaling, we examined transcription factors that mediate responses to auxin, which has effects on root development, and cytokinin, which mediates nitrogen responses (13). We found a total of four cytokinin-responsive transcriptional activators (B type ARRs), four cytokinin signaling inhibitors (A type ARRs), six auxin response factors (ARFs), and seven auxin/indole-3-acetic acid inducible genes (Aux/IAAs) whose expression was well correlated with the largest cell-specific response clusters in pericycle and lateral root cap. These hormone responses provide two sets of candidate upstream activators and
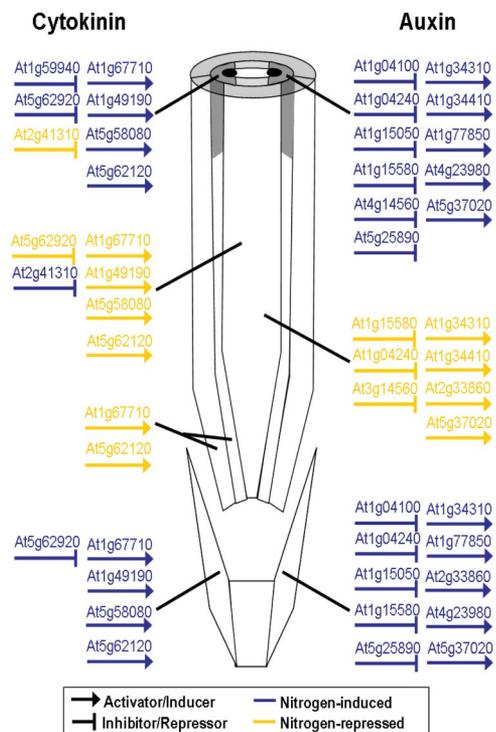
Fig. 2. Hormones are candidate signaling cues for cell-specific nitrogen responses. Transcriptional regulators of cytokinin and auxin signals show a highly cell-specific response pattern. Cell types or tissues in which regulation was observed are outlined in black (lateral root cap, endodermis/pericycle, stele) with pericycle founder cells highlighted (gray cells adjacent to black ovals representing xylem poles). The cell-specific regulation patterns of the hormone response regulators are (cluster designation in parentheses): ARR type B positive cytokinin regulators At1g67710 (16), At1g49190 (12), At5g58080 (12), At5g62120 (16); ARR type A negative cytokinin regulators At1g59940 (4), At2g41310 (23), At3g57040 (1), At5g62920 (12); ARFs At1g34310 (12), At1g34410 (5), At1g77850 (13), At2g33860 (11), At4g23980 (13), At5g37020 (12); Aux/IAAs At1g04240 (12), At1g04100 (13), At1g15050 (13), At1g15580 (12), At3g23030 (1), At4g14560 (5), and At5g25890 (13). The two genes in the constitutive response category (cluster 1) are not shown. The number of genes in each cell type is represented with the appropriate number of arrow symbols; each arrow is colored to designate nitrogen regulation of the gene, shaped to distinguish gene function as an activator/inducer or inhibitor/repressor and labeled with the *Arabidopsis* Genome Initiative (AGI) ID.

negative feedback mechanisms that could coordinate nitrogen responses in the same cells (Fig. 2). These data also provide a resource to explore how hormone signals can elicit different effects in different tissues, a critical question in hormone response.

For example, responses that occurred in pericycle founder cells are particularly interesting, because these cells will eventually mediate a dramatic change in root architecture under long-term exposure to treatment conditions (Fig. 3). Indeed, cellular response profiles suggested that, within the 3.5-h treatment, changes in lateral root regulation had occurred because *PLETHORA1* (*PLT1*), which is expressed discretely in initiating lateral roots within the pericycle (14, 15), was sharply up-regulated in pericycle founder cells (Fig. 1a, cluster 12).

MicroRNA Mediates a Pericycle-Specific Response to Nitrogen. To demonstrate that the genome-wide responses we uncovered are relevant to environmental response, we analyzed in detail one case study to determine whether predictions from the cell-sorting data were supported by genetic and phenotypic analysis. We focused on the validation of the nitrogen-regulated pericycle
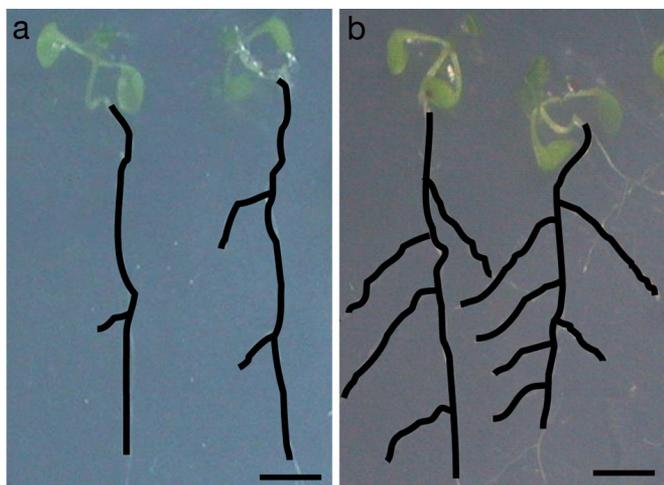
Fig. 3. Root architecture is highly plastic in response to different levels of nitrogen. (*a* and *b*) Twelve-day-old seedlings grown continually on (*a*) 5 mM nitrate or (*b*) 0.5 mM ammonium succinate. (Scale bars, 1 cm.)

response as potentially mediated by *ARF8*, which was one of the pericycle-induced *ARF*s and is itself a documented target of microRNA 167 (miR167) (16). Thus, *ARF8* offers a link between environmental inputs and auxin-mediated plasticity of lateral root architecture.

ARF8 has been shown to have developmental roles in the shoot (16) and subtle phenotypes in root (17) but was not previously known to be a regulator of developmental plasticity. To test the hypothesis that *ARF8* regulates lateral roots in response to nitrogen, we first confirmed that *ARF8* is nitrogen-induced in the pericycle (Fig. 4 *a–c*) and lateral root cap (data not shown) using qPCR and reporter constructs expressing *ARF8* gDNA fused to *GUS* cDNA under the *ARF8* promoter (16) in whole roots. Statistical analyses show that *ARF8* is also repressed in the stele, suggesting that, whereas it is induced in the pericycle, it is repressed in the xylem and phloem. We found that miR167a,b was expressed specifically in the pericycle and lateral root cap along with *ARF8*, but, consistent with an antagonist effect on *ARF8*, was repressed in the pericycle and lateral root cap in response to nitrogen, as determined by qPCR of both the mature miR167a/b and the miR167a precursor and staining intensity of a $P_{MIR167a}$::*GUS* reporter (16) (Fig. 4 *d–f* and *j*). We used qPCR of premiR160a and mature miR160a/b as a non-nitrogen-regulated miR control, showing no response (SI Table 6). An *ARF8*:*GUS* fusion with a mutated miR167-binding site (m*ARF8*:*GUS*) (16) showed loss of nitrogen regulation (Fig. 4 *g–i*). In conjunction with previous results showing that miR167a targets *ARF8* (16), these results show that nitrogen represses levels of miR167a to permit the *ARF8* transcript to accumulate in the pericycle upon nitrogen treatment.

The ARF8 Circuit Controls Lateral Root Architecture. We next asked whether the *ARF8*/miR167 circuit was involved in mediating the observed long-term effects of our nitrogen treatment on lateral root outgrowth, using genetic backgrounds with perturbed levels of miR167a and *ARF8* (16). Because the pericycle GFP line that we used marks both initiating and preemergent lateral roots (Fig. 4*k*), it seemed feasible that the *ARF8*/miR167 circuit controlled a potential checkpoint between lateral root initiation and subsequent emergence (18, 19). In wild-type (Col-0) plants, nitrogen treatment led to an increased ratio of initiating vs. emerging lateral roots (Fig. 4*l*; $\chi^2 P = 8$–13E), a strategy that apparently enables plants to initiate lateral roots in high nitrogen conditions but stimulates lateral root outgrowth to "forage" the soil for

nutrients only in nitrogen-depleted conditions. This strategy also explains why *PLT1* induction suggested increased lateral root initiation whereas the long-term treatments led to fewer emergent lateral roots. The apparently subtle effect observed over 4 days of nitrogen treatment accumulated over longer treatments, to lead to dramatic changes in root architecture, such as observed after 12 days (e.g., Fig. 3).

In contrast to wild-type plants, *P35S*::*MIR167a* seedlings that overexpress miR167a exhibited a complete loss of nitrogen control over lateral root emergence (Fig. 4*l*; $\chi^2 P = 0.5354$). *arf8* roots also show a lack of nitrogen control over emergence ($\chi^2 P = 0.1369$), although some nitrogen response may persist perhaps due to redundancy with *ARF6*, which is also a target of miR167a (16). Together, these results show how a cell-specific response circuit controls a major aspect of the plant's strategic response to nitrogen influx via changes in root architecture. The result also demonstrates how quantitative adjustments in transcriptional circuits (*ARF8* and miR167) can ultimately lead to changes in root architecture over time.

The Putative ARF8 Module Is Regulated by Glutamine. To explore factors downstream of the miR167-*ARF8* circuit in the pericycle, we tested whether potential *ARF8* targets exhibit coordinated responses within the pericycle. To build such a list of potential targets, we searched for genes that were induced in the pericycle (where *ARF8* induction is most dramatic), that had an ARF-binding site, and that also showed moderate correlation ($R \geq 0.5$) with *ARF8* over $\approx 1,900$ microarray experiments deposited in the NASC database (20) (SI Text). The procedure identified 126 potential targets (SI Table 8).

To test whether the putative *ARF8* module formed a cohesive response group, we asked whether *ARF8* and the 126 potential targets responded similarly to either nitrate or downstream metabolites. Thus, we treated roots with nitrate and methionine sulfoximine (MSX), which blocks the assimilation of nitrate into glutamine (Gln) and consequently glutamate (21), and collected pericycle cells for RNA analysis. Induction of *ARF8* and all 126 of the putative *ARF8* targets was blocked by MSX treatment ($q < 5\%$ FDR), suggesting they were responsive to downstream nitrogen metabolites rather than nitrate itself (Fig. 4*m*). To confirm that the effect was specific to metabolite signaling, we repeated the MSX block of nitrate metabolism into glutamate/glutamine, but added glutamine, which should restore metabolite signaling if the signal is glutamine or a derived nitrogen metabolite. The induction of *ARF8* and all 126 of the putative *ARF8* targets was indeed restored by the glutamine "add back" ($q < 5\%$ FDR) (Fig. 4*m*). No other *ARF*s that were induced in the pericycle showed the same coordinated regulation with this cluster. Overall, the data are consistent with *ARF8* and its putative pericycle targets forming a cohesive response module under coordinated regulation by glutamine or a downstream metabolite (Fig. 4*n*).

Discussion

Taken together, these results demonstrate a link between microRNA regulation and nitrogen responses, as has been shown with phosphate and sulfate (22, 23). Importantly, this proof of principle demonstrates that profiling cellular responses provides a trail of evidence that leads directly to discrete, highly compartmentalized circuits that, in turn, mediate cell-specific functions.

Interestingly, our finding that glutamine/glutamate is the predominant signal regulating repression of lateral root emergence is in contrast to an earlier report showing lateral root development is enhanced in a nitrate reductase mutant (24), suggesting that nitrate accumulation rather than glutamine/glutamate in fact plays an important role in this process. In one previous study, glutamine treatment also resulted in some lateral

Fig. 4. Antagonistic regulation between miR167a and *ARF8* in response to nitrogen mediates lateral root initiation and emergence. (*a*, *d*, and *g*) GUS-stained control roots. (*b*, *e*, and *h*) GUS-stained nitrogen-treated roots; all roots were GUS-stained for 12 h. (*c*, *f*, and *i*) Average expression level of indicated genes and constructs assessed by qPCR in whole roots control- (C) or nitrate-treated (T) from three biological replicates. (*a–c*) Nitrogen induction of *gARF8:GUS* and qPCR quantification of *ARF8* expression. (*d–f*) Nitrogen repression of $P_{MIR167a}$::*GUS* and qPCR quantification of premiR167a expression. A control microRNA (miR160) showed no nitrogen response (SI Table 6). (*g–i*) Loss-of-nitrogen induction of *ARF8* expression in *mARF8:GUS* and qPCR quantification of GUS expression. (*j*) Response of mature miR167a/b to nitrogen treatment in the five cell populations profiled. (*k*) Confocal images of initiating and preemergent lateral roots (GFP-marked) and emerging lateral roots (not GFP-marked) in the line used for cell sorting that marks pericycle cells adjacent to the xylem pole (E3754). (*l*) Bar graphs show the relative mean percentages of initiating (light-colored bars) and emerging (dark-colored bars) lateral roots in Col-0, *arf8*, and *P35S*::*MIR167a* 4 days after 12-day-old seedlings were either mock- (no treatment) or nitrogen-treated; see SI Table 7 for actual values. To the right of the bars, the average number of lateral roots per seedling is shown. The *P35S*::*MIR167a* has fewer lateral roots in total as a consequence of having shorter roots. (*m*) Heat map showing the response (blue, induction; yellow, repression) of *ARF8* and the 126 predicted target genes in the putative *ARF8* module to nitrate (treat), KCl (control), MSX, and Gln treatments in sorted pericycle founder cells. (*n*) Summary of the miR167/*ARF8*-regulated genetic circuitry that controls the balance between initiating and emerging lateral roots in relation to nitrogen availability. (Scale bars, 25 μm.)

root inhibition in agreement with glutamine playing a signaling role. In addition, the previous work focused on repression of the elongation of lateral roots postemergence, whereas we studied the nitrogen effect on the balance between initiation/preemergence and emergent lateral roots, which has been defined as a critical developmental checkpoint (25). The two results suggest that different signals predominantly regulate lateral root establishment vs. elongation, a strategy that may help the plant fine-tune its developmental response to nutrients.

Overall, we show that dynamic profiling of cell types increases both sensitivity to detect highly localized responses to environmental signals and resolution to distinguish distinct functional modules within cells. We believe this technique reveals an aspect of nitrogen signaling that has been largely undetected in the superimposition of pathways from mixed tissue samples. It is likely that a similar scale of cell-specific responses occurs in reaction to many inputs in both plants and animals. In principle, cellular profiling can be used with a diverse set of inputs, including developmental time series and other environmental inputs. Thus, dynamic profiling of cells should lead to new insights about how organs fine-tune their plasticity to the environment.

Materials and Methods

Plant Material. *Arabidopsis* GFP lines were selected to mark the lateral root cap (E4722), epidermis and cortex (E1001), endodermis and pericycle (E470), pericycle (E3754) (SI Fig. 5) (obtained from http://enhancertraps.bio.upenn.edu), and the stele (*pWOL*::*GFP*) (26). ARF8 and miR167-related lines *gARF8:GUS*, *mARF8:GUS*, $P_{MIR167a}$::*GUS*, *arf8-3*, and T1 transformants expressing *P35S*::*MIR167a* were obtained from the Reed laboratory (16). *ATGSR1:GFP* was from (9). All lines were in the Col-0 background.

Plant Growth and Treatment. We chose our growth conditions and nitrogen treatments based on previous studies and used qPCR to reconfirm previously observed nitrogen responses (data not shown) (7, 10, 11). The growth conditions were chosen to deplete nitrogen before treatment but to avoid nitrogen starvation that could cause potential stress responses. To do this, plants were grown in a low nitrogen environment using a low level of ammonium succinate as an alternative source of nitrogen to nitrate (10, 11) and the ammonium levels monitored over time. The experiment was carried out with two different numbers of seeds (either 1,500, as required for microarray experiments, or 300, as required for phenotypic experiments) and under a range of initial

ammonium succinate concentrations. We determined appropriate ammonium succinate concentrations for different growth setups by testing a series of different concentrations for signs of stress in plants at different time points, noting the point when plants showed signs of stress, and by monitoring depletion using an ammonium assay. For a standard 12-day growth period, we determined that concentrations of 0.5 mM ammonium succinate for 1,500 seeds and 0.2 mM ammonium succinate for 300 seeds led to reduced but not entirely depleted ammonium in the media. No signs of nitrogen starvation/stress were evident in these seedlings.

All experiments were carried out in triplicate. Approximately 6,000 seeds (per replicate) of each GFP line for sorted cell experiments or of Col-0 for whole-root and protoplast treatment controls were sterilized and sown on Nitex 03–250/47 mesh (Sefar America). The mesh was supported on a plastic platform to allow roots to grow in hydroponics inside a sterile Phytatray (Sigma–Aldrich); 1,500 seeds were sown in each Phytatray. Growing media consisted of $1\times$ Murashige and Skoog basal medium containing no nitrogen or sucrose (custom-ordered, GibcoBRL, Gaithersburg, MD) supplemented with 3 mM sucrose and 0.5 mM ammonium succinate. All components were kept sterile throughout the growth period of a 16-h light (50 mmol photons m^{-2}s^{-1} light intensity)/8-h dark cycles at 22°C, which was maintained inside a growth incubator (Percival Scientific). For treatments, KNO$_3$ was added to the media to a final concentration of 5 mM for 2 hours at the start of the light period on

day 12 (7, 11). Control plants were mock-treated by adding the same concentration of KCl. For MSX treatments, we used 5 mM KNO$_3$ or 5 mM KCl and 1 mM MSX or 1 mM MSX plus 5 mM glutamine (Gln), as described (21). For qPCR and phenotypic tests in different genetic backgrounds, 300 seeds of each *ARF8*- and miR167-related line and Col-0 in *ARF8*/miR167 experiments were treated in a similar fashion but were grown on 0.2 mM ammonium succinate.

ANOVA. The two-way ANOVA was modeled as follows: $Y = \mu + \alpha_{\text{cell pop}} + \alpha_{\text{treatment}} + \alpha_{\text{cell pop* treatment}} + \varepsilon$, where Y is the normalized dChip expression signal of a gene; μ is the global mean; the α coefficients correspond to the effects of cell population, treatment; and the interaction between cell population and treatment, and ε represents unexplained variance.

1. Birnbaum K, Shasha DE, Wang JY, Jung JW, Lambert GM, Galbraith DW, Benfey PN (2003) *Science* 302:1956–1960.
2. Birnbaum K, Jung JW, Wang JY, Lambert GM, Hirst JA, Galbraith DW, Benfey PN (2005) *Nat Methods* 2:615–619.
3. Roy PJ, Stuart JM, Lund J, Kim SK (2002) *Nature* 418:975–979.
4. Vitousek PM, Howarth RW (1991) *Biogeochemistry* 13:87–115.
5. Little DY, Rao H, Oliva S, Daniel-Vedele F, Krapp A, Malamy JE (2005) *Proc Natl Acad Sci USA* 102:13693–13698.
6. Remans T, Nacry P, Pervent M, Filleur S, Diatloff E, Mounier E, Tillard P, Forde BG, Gojon A (2006) *Proc Natl Acad Sci USA* 103:19206–19211.
7. Gutierrez RA, Lejay LV, Dean A, Chiaromonte F, Shasha DE, Coruzzi GM (2007) *Genome Biol* 8:R7.
8. Tusher VG, Tibshirani R, Chu G (2001) *Proc Natl Acad Sci USA* 98:5116–5121.
9. Tian GW, Mohanty A, Chary SN, Li S, Paap B, Drakakaki G, Kopec CD, Li J, Ehrhardt D, Jackson D, *et al.* (2004) *Plant Physiol* 135:25–38.
10. Wang R, Okamoto M, Xing X, Crawford NM (2003) *Plant Physiol* 132:556–567.
11. Wang R, Tischner R, Gutierrez RA, Hoffman M, Xing X, Chen M, Coruzzi G, Crawford NM (2004) *Plant Physiol* 136:2512–2522.
12. Vieten A, Sauer M, Brewer PB, Friml J (2007) *Trends Plants Sci* 12:160–168.
13. Sakakibara H, Takei K, Hirose N (2006) *Trends Plants Sci* 11:440–448.
14. Aida M, Beis D, Heidstra R, Willemsen V, Blilou I, Galinha C, Nussaume L, Noh YS, Amasino R, Scheres B (2004) *Cell* 119:109–120.
15. Blilou I, Xu J, Wildwater M, Willemsen V, Paponov I, Friml J, Heidstra R, Aida M, Palme K, Scheres B (2005) *Nature* 433:39–44.
16. Wu MF, Tian Q, Reed JW (2006) *Development* 133:4211–4218.
17. Tian CE, Muto H, Higuchi K, Matamura T, Tatematsu K, Koshiba T, Yamamoto KT (2004) *Plant J* 40:333–343.
18. Malamy JE (2005) *Plant Cell Environ* 28:67–77.
19. Walch-Liu P, Ivanov I, Filleur S, Gan Y, Remans T, Forde BG (2006) *Ann Bot (Lond)* 97:875–881.
20. Craigon DJ, James N, Okyere J, Higgins J, Jotham J, May S (2004) *Nucleic Acids Res* 32:D575–577.
21. Rawat SR, Silim SN, Kronzucker HJ, Siddiqi MY, Glass AD (1999) *Plant J* 19:143–152.
22. Chiou TJ (2007) *Plant Cell Environ* 30:323–332.
23. Bari R, Datt Pant B, Stitt M, Scheible WR (2006) *Plant Physiol* 141:988–999.
24. Zhang H, Jennings A, Barlow PW, Forde BG (1999) *Proc Natl Acad Sci USA* 96:6529–6534.
25. Malamy JE, Benfey PN (1997) *Development* 124:33–44.
26. Bonke M, Thitamadee S, Mahonen AP, Hauser MT, Helariutta Y (2003) *Nature* 426:181–186.

Gifford *et al.*